ISSN 1063-7834, Physics of the Solid State, 2009, Vol. 51, No. 4, pp. 817–822. © Pleiades Publishing, Ltd., 2009.
Original Russian Text © S.V. Mel'nikova, A.S. Krylov, A.L. Zhogal', N.M. Laptash, 2009, published in Fizika Tverdogo Tela, 2009, Vol. 51, No. 4, pp. 771–776.

LATTICE DYNAMICS AND PHASE TRANSITIONS

Optical Studies of Phase Transitions in the $(NH_4)_3Ti(O_2)F_5$ Crystal

S. V. Mel'nikova[a]*, A. S. Krylov[a], A. L. Zhogal'[a], and N. M. Laptash[b]**

[a] *Kirensky Institute of Physics, Siberian Branch, Russian Academy of Sciences, Akademgorodok, Krasnoyarsk, 660036 Russia*
**e-mail: msv@iph.krasn.ru*

[b] *Institute of Chemistry, Far East Division, Russian Academy of Sciences, pr. Stoletiya Vladivostoka 159, Vladivostok, 690022 Russia*
***e-mail: laptash@ich.dvo.ru*

Received July 7, 2008

Abstract—Polarization-optical study of twinning and measurements of the Raman spectra and birefringence in oxyfluoride $(NH_4)_3Ti(O_2)F_5$ were carried out over the temperature range 90–350 K. Phase transitions were detected at temperatures T_{01} = 266 K (second-order transition) and T_{02} = 225 K (first order). It is assumed that the crystal symmetry is changed as follows: $Fm3m \longleftrightarrow I4/mmm \longleftrightarrow I4/m$. Anomalies of the spectral parameters are established in the frequency range of internal vibrations of ammonium ions and $Ti(O_2)F_5$ complexes. An analysis of the results shows that the transition at T_{01} is likely due to small shifts of the tetrahedral groups from their position on the triad axis and that the transition at T_{02} is due to fluorine–oxygen ordering of $Ti(O_2)F_5$ complexes.

PACS numbers: 64.70.Kb, 61.72.Mm, 78.20.Fm, 78.30.Hv

DOI: 10.1134/S1063783409040301

1. INTRODUCTION

In the numerous family of crystals with the elpasolite–cryolite structure in which the octahedron MX_6 (M = Al, Fe, Ti, Zr, Nb, Mo, W; X = O, F, Cl) is the main building block, the group of compounds with seven-coordinated complexes MX_7 have attracted considerable research interest. Among them are crystals $(NH_4)_5HfF_7$, $(NH_4)_3ZrF_7$, $(NH_4)_3NbOF_6$, and many others. The authors of [1–4] believe that the structures of these compounds are built of complexes in the form of misoriented pentagonal bipyramids. In [5], the structure of the oxyfluoride $(NH_4)_3Ti(O_2)F_5$ crystal was considered from the same standpoint. However, the authors of [6, 7] believe that, at room temperature, the (O_h^5–$Fm3m$)-disordered peroxyfluoride complex $Ti(O_2)F_5$ is an octahedron and the two oxygen atoms form, due to their short bond, an O–O dumbbell, which statistically occupies one of the octahedron vertices and is oriented perpendicular to the fourfold axis in two equally probable positions. The ammonium ions occupy two nonequivalent crystallographic positions in the cubic unit cell. In one of the positions, the ions are in interoctahedral voids on the triad axes and have only a single orientation, according to the symmetry of the site they occupy. In another position, the ammonium ions are inside octahedral voids and can have at least six or eight different orientations.

The study of the heat capacity of this material in [7] showed the occurrence of a first-order structural phase transition (PT) at T_0 = 226 K. The PT is accompanied by a jumpwise splitting of X-ray reflections indicating a lowering of the crystal symmetry. However, the symmetry of the low-temperature phase of the material was not established. Apart from the aforementioned results, it was detected in [7] that the behavior of the heat capacity and the integrated characteristics of the structural transformations in $(NH_4)_3Ti(O_2)F_5$ samples are dependent on the crystallization conditions. For example, the anomaly of the temperature dependence of the excess heat capacity $\Delta C_p(T)$ characteristic of crystals grown with a high rate (samples A) is a wide hill with a sharp peak on the right-hand shoulder. At the same time, the anomaly of the heat capacity of slowly grown samples (B) is a nearly symmetric sharp peak. The enthalpies of the corresponding thermal effects in samples of different crystallizations are different: $\Sigma\Delta H_i$ = 700 J/mol K in samples A and ΔH_0 = 1800 J/mol K in samples B.

In this work, we carried out polarization-optical studies and measurements of birefringence and the Raman spectra over the temperature range 90–350 K in order to determine the symmetry of the $(NH_4)_3Ti(O_2)F_5$ crystal in the low-temperature range and the involvement of different building blocks in the structural rearrangement during the phase transition.

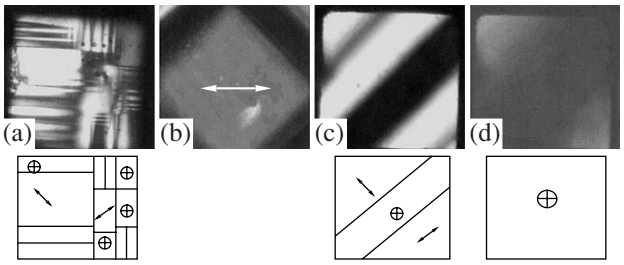

Fig. 1. Twin patterns and schematic diagrams of twinning of the $(NH_4)_3Ti(O_2)F_5$ crystal in the various phases: (a) phase G_1 during cooling, (b) extinction position in phases G_1 and G_2, (c) phase G_2, and (d) phase G_1 on heating. In the diagrams, double-headed arrows indicate the extinction position in twins and circles show the optical axis intersecting the surface.

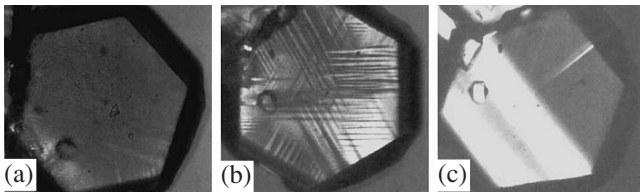

Fig. 2. Polarized-light images of a $(111)_c$ plate of the $(NH_4)_3Ti(O_2)F_5$ crystal at (a) $T = 260$ K (nucleation of G_1-phase twins at the plate edges), (b) $T = 226$ K (phase G_1), and (c) $T = 200$ K (phase G_2).

2. EXPERIMENTAL

The $(NH_4)_3Ti(O_2)F_5$ compound was synthesized in a solution according to the reaction

$$(NH_4)_2TiF_6 + NH_4F + H_2O_2 = (NH_4)_3Ti(O_2)F_5 + 2HF.$$

An excess of NH_4F and a concentrated solution of H_2O_2 were added to a $(NH_4)_2TiF_6$ solution. As a result, an ample sediment of $(NH_4)_3Ti(O_2)F_5$ of yellow-lemon color consisting of fine (~10 μm) octahedral single crystals (samples *A*) was formed. After separation of this sediment from the solution and subsequent slow evaporation, coarser bright-yellow single crystals (samples *B*) were formed. Perfect octahedra with a cut $(100)_c$ vertex did not exceed 100–200 μm in size. The largest crystals were $(111)_c$ plates obtained through the growth of an octahedron face with an edge size of 200–2000 μm. On such samples, we performed polarization-optical studies using an Axiolab polarizing microscope and measured the birefringence Δn (using a Berec compensator) and the Raman spectra. The results presented below were obtained on the largest uniform samples of crystallization *B*. Neither the Raman studies nor the polarization-optical observations (as far as the crystal sizes of the first crystallization allowed) detected any difference between samples *A* and *B*.

The Raman spectra were measured in the range 15–3500 cm^{-1} on a T64000 triple spectrometer (Jobin Yvon, France) with a CCD detector in the dispersion subtractive mode. The entrance slit was 100 μm in size, which corresponds to a resolution of about 2 cm^{-1}. The spectra were excited by a 100-mW Ar^+ laser (wavelength, 514.5 nm). The exposure time was 20 s. In order to decrease noise, the data were averaged over ten measurements. The spectrum excitation and collection of the scattered light were performed using a microscope supplied with an objective with 50-fold magnification; the analyzed area was ~5 μm in size. In the temperature studies, we used a THMS-600 camera (Linkam, UK). Quantitative information on the parameters of the spectral lines was obtained by mathematical processing using a Voigt spectral profile.

The studies in polarized light show that, at room temperature, the crystal is indeed cubic (phase G_0). On cooling somewhat below the ice melting temperature (at $T_{01} \approx 270$ K), we unexpectedly detected a distortion of the optical isotropy and the formation of a regular twin structure. In a $(100)_c$ plate, striped twins are visualized having boundaries along $[110]_c$. As the microscope stage is rotated, extinction of some twins is observed along $[100]_c$, then they become bright, but the others remain dark (Figs. 1a, 1b). A second-order phase transition occurs at T_{01}, which is accompanied by a change in the crystal system (phase G_1). Below the phase transition at $T_{02} = 225$ K established earlier [7], the twinning pattern is sharply changed: the motion of a phase front is observed, the illumination intensity is changed, and a color appears. The twins become coarse (Fig. 1c), and the boundaries are formed along $[100]_c$; however, the state of extinctions in different twins remains unchanged (Fig. 1b) (phase G_2). The dark twin (for which the optical axis intersects the crystal surface) is the largest. During repeated experiments, this twin can occupy the entire sample volume and remain the same in the G_1 phase during heating (Fig. 1d).

Observations of a $(111)_c$ cut (Fig. 2a) show that, below the temperature T_{01}, the structure of the sample has three types of twin boundaries arranged at 120° to each other. On the transition at T_{02}, the light intensity and interference color are sharply changed, the twins become significantly coarser, and new boundaries are formed (Fig. 2b). The presence of sufficiently large twin regions allowed us to measure the temperature dependence of the birefringence in a $(111)_c$ plate (Fig. 3). It is seen that optical anisotropy arises smoothly below T_{01} and then increases linearly. At T_{02}, the birefringence increases in a jumpwise manner and increases gradually to a maximum and then decreases during further cooling.

Figure 4 presents the Raman spectrum of the $(NH_4)_3Ti(O_2)F_5$ crystal measured at room temperature ($T = 293$ K). The lines below ~700 cm^{-1} correspond to stretching vibrations of the Ti–F bonds and deformation modes of the $Ti(O_2)F_5$ ion complexes. In the range 800–950 cm^{-1}, there are bands corresponding to

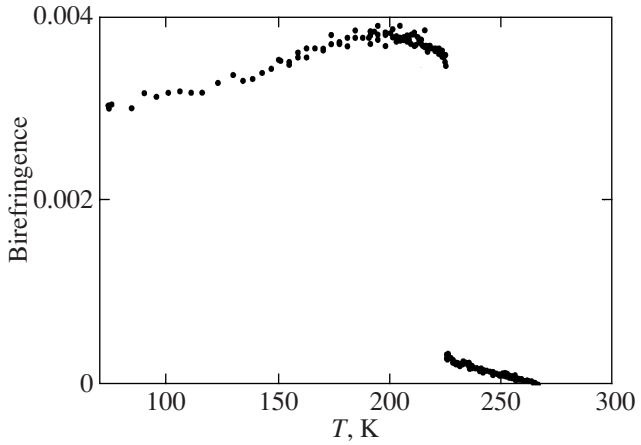

Fig. 3. Temperature dependence of the birefringence in the $(NH_4)_3Ti(O_2)F_5$ crystal measured in a $(111)_c$ plate.

stretching vibrations of the Ti–(O_2) bond in the complex, and the line at 901 cm^{-1} belongs to the fully symmetric stretching vibration of the Ti–(O_2) bond.

The ranges 1200–1800 and 2700–3500 cm^{-1} contain lines belonging to deformation and internal stretching vibrations of the ammonium ions, respectively. The lines are markedly broadened and split even in the cubic phase, and their frequencies (2841, 3070, and 3190 cm^{-1} for the stretching vibrations and 1413, 1450, and 1688 cm^{-1} for the deformation vibrations) are close to the frequencies of the internal vibration modes of the free ion [8]. The shift in their frequencies and the splitting of the lines indicate that the ammonium ions are distorted by the crystalline surroundings and weakly interact with each other.

At room temperature, a central peak is observed at low frequencies. As the temperature decreases, this peak disappears. A large number of narrow lines (approximately up to 150 cm^{-1}) belong to the spectrum of air, which we failed to remove in the geometry of the experiment.

As the temperature decreases, the most substantial changes occur near the phase transition point T_{02} in the group of lines at ~600 and ~900 cm^{-1}. The detailed temperature dependence of the line profile of the fully symmetric stretching vibration of the Ti–(O_2) bond is shown in Fig. 5. It is well seen that, even in the cubic phase, there are at least two lines, at 902 and 892 cm^{-1}. However, the intensity of the latter is very low, and it is manifested only in the profile asymmetry during the mathematical processing. The inset to Fig. 5 shows the temperature dependence of the ratio of the line intensities at 902 and 892 cm^{-1}. On cooling, the intensity of the line at 892 cm^{-1} increases monotonically and both the lines exhibit almost equal intensity below the phase transition point T_{02} = 225 K. The transition is accompanied by a jumpwise change in the position of the lines. However, the distance between them remains almost unchanged as the temperature decreases. In the range of the ammonium vibrations, as the temperature decreases below T_{02}, the lines narrow and become better resolved, but there are no anomalous variations in the spectral parameters.

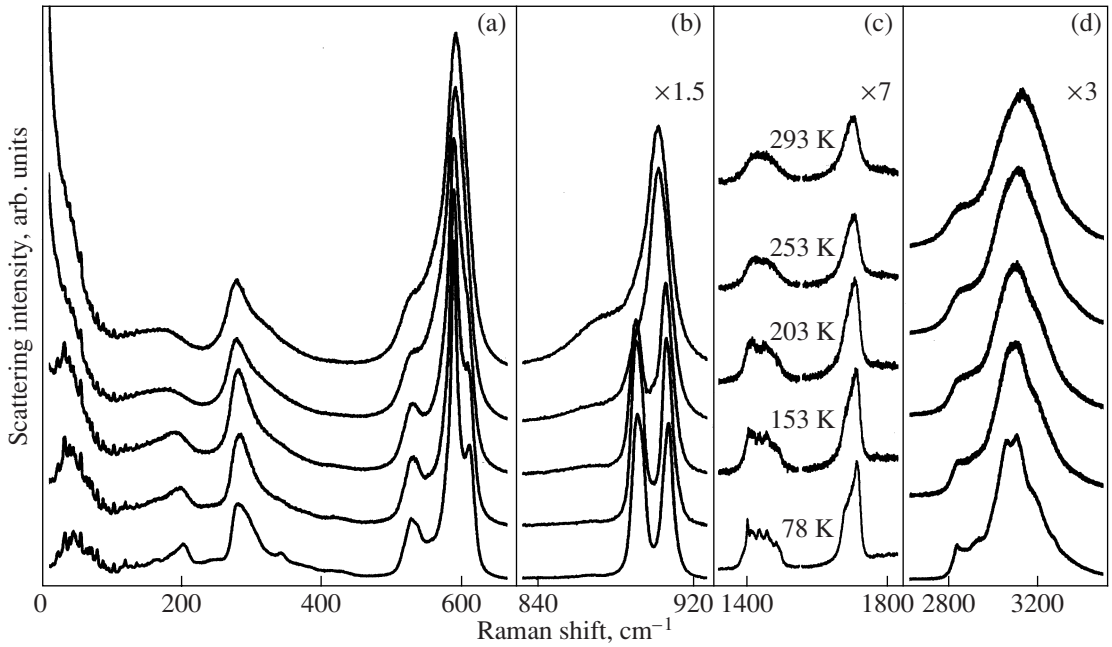

Fig. 4. Raman spectrum of the $(NH_4)_3Ti(O_2)F_5$ crystal measured at room temperature (293 K) and its transformation with temperature: (a) the low-frequency range with a central peak on the left, deformation modes of the $Ti(O_2)F_5$ complex, and stretching vibration modes of the Ti–F bonds; (b) stretching vibrations of the Ti–(O_2) bond of the complex; and (c, d) deformation and internal stretching vibration modes of the ammonium ions, respectively.

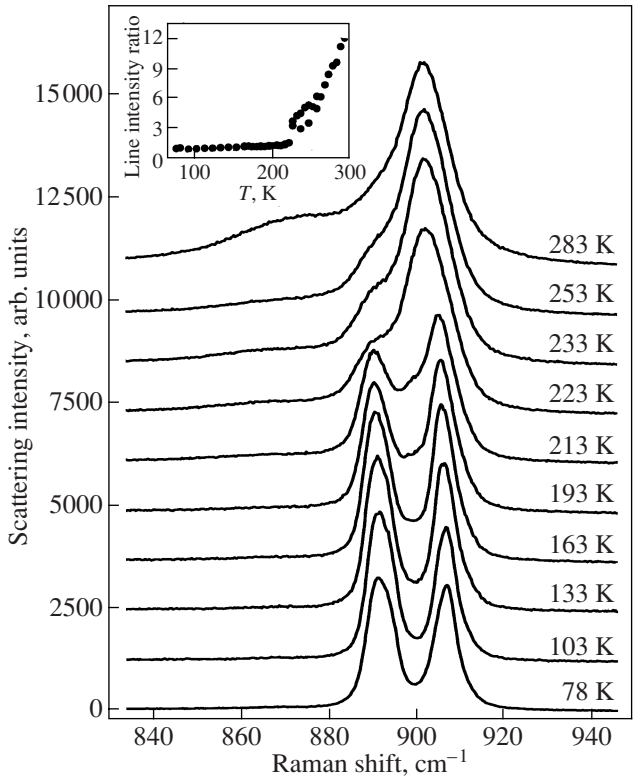

Fig. 5. Transformation of the spectral line of the fully symmetric Ti–(O_2) stretching vibration mode with temperature. The inset presents the temperature dependence of the ratio of the line intensity at 902 cm^{-1} to that at 892 cm^{-1}.

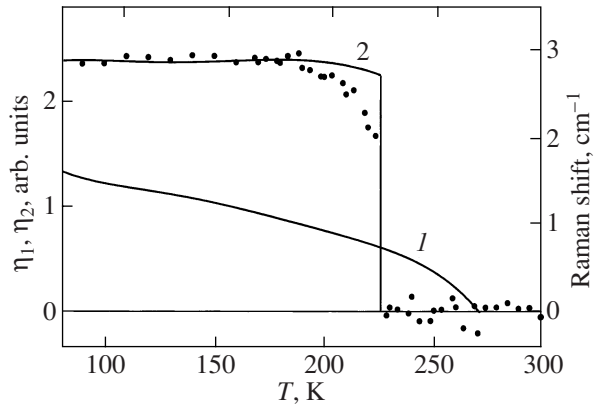

Fig. 6. Temperature dependences of the phase-transition order parameters (*1*) η_1 and (*2*) η_2 calculated from the birefringence. Points indicate the anomalous portion of the frequency shift of the line at 902 cm^{-1} with temperature.

3. DISCUSSION OF THE RESULTS

Thus, the polarization-optical observations and measurements of birefringence allowed us to establish the existence in the $(NH_4)_3Ti(O_2)F_5$ crystal of two structural transitions with the following sequence of phase changes: $G_0 \longleftrightarrow G_1 \longleftrightarrow G_2$. The appearance of three types of twin boundaries in a $(111)_c$ cut below T_{01} demonstrates that the crystal loses its triad axis. In a $(100)_c$ plate, there are twins in which the optical axis intersects the surface. The second-order transition from the cubic (G_0) to tetragonal (G_1) phase occurs with the loss of the triad axes. On further cooling, in spite of the appearance of new twin boundaries in phase G_2, its symmetry remains tetragonal, as is demonstrated by the existence of a twin in which the optical axis of the uniaxial crystal intersects the surface. The appearance of new twin boundaries indicates an additional loss of symmetry elements at T_{02}.

Since the optical indicatrix is not rotated in the tetragonal phases, the birefringence appearing in the G_1 phase is proportional to the squared order parameter: $\Delta n(T) \sim \eta_1^2 \sim (T_{01} - T)^{2\beta}$. The linear temperature dependence of the birefringence in the G_1 phase shows that the exponent in the temperature dependence of the order parameter is $\beta = 0.50 \pm 0.01$. This value is characteristic of second-order transitions far from the tricritical point. From the intercept of the linear dependence, the phase-transition temperature is refined to be $T_{01} = 266$ K. We assume that the structural transformation at T_{01} is due to small displacements of the tetrahedral groups located on the body diagonals of the cubic lattice, which might cause the loss of the triad axes. It is known that, on such transformations, the jump in the heat capacity is small (for the ferroelastic PT in $RbMnCl_3$, $\Delta C_p \approx 3.5$ J/mol K [9]); Thus, such a thermal anomaly might remain undetected in the experiment [7].

According to our polarization-optical studies, the first-order phase transition at $T_{02} = 225$ K established earlier [7] is not accompanied by a change in the crystal system. The crystal lattice remains tetragonal, but the transition is accompanied by the loss of some symmetry elements. Based on the data from [7] indicating the absence of a superstructure over the entire temperature range studied and the results of this work, we derived the possible symmetry of the phases of this crystal assuming that the center of symmetry persists in all the phases. Based on group-theoretical analysis [10], the sequence of transitions $G_0 \longleftrightarrow G_1 \longleftrightarrow G_2$ can be characterized as follows: $Fm3m \longleftrightarrow I4/mmm \longleftrightarrow I4/m$. In the latter transition, an additional order parameter η_2 arises in a jumpwise manner. The unusual behavior of the birefringence in the low-temperature G_2 phase is due to the influence of both the parameters: $\Delta n(T) \sim (\eta_1 + \eta_2)^2$. Extrapolating the linear run of $\Delta n(T)$ from phase G_1 to phase G_2, we determine the contribution from the parameter η_1 to the total birefringence and the contribution due to the parameter η_2. Figure 6 shows the calculated temperature dependences of both the parameters in arbitrary units. The $\eta_2(T)$ dependence shows that the transition at T_{02} is a pronounced first-order transition. Figure 6 also shows the temperature dependence of the frequency shift of the Raman spectral line at 902 cm^{-1}. The exper-

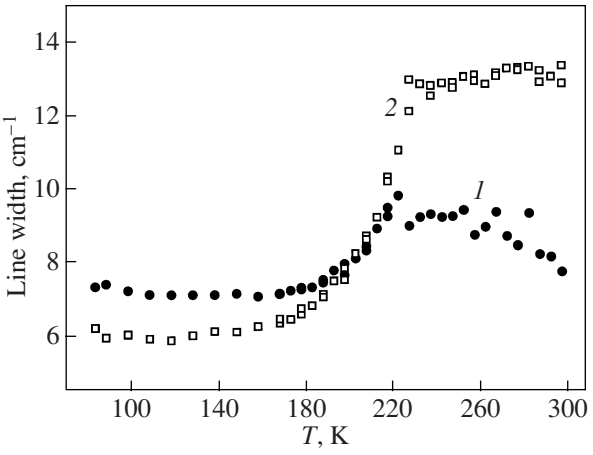

Fig. 7. Temperature dependence of the linewidth of the vibrations at (*1*) 892 and (*2*) 902 cm^{-1}.

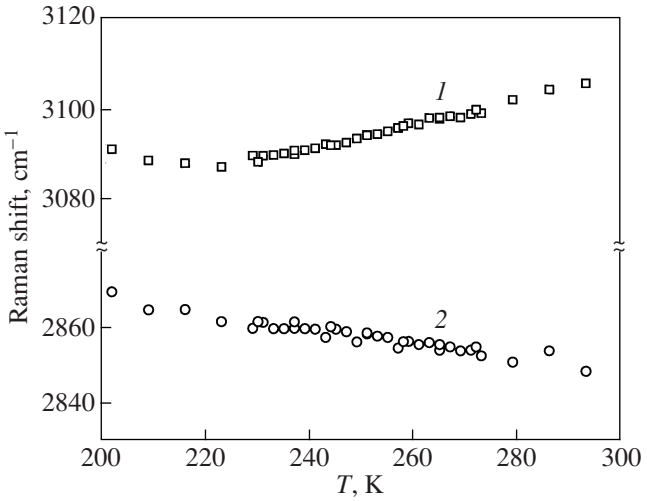

Fig. 8. Temperature dependence of the frequency of the stretching vibration modes of the ammonium group at (*1*) 3100 and (*2*) 2840 cm^{-1}.

imental and calculated $\eta_2(T)$ dependences are seen to be similar. This fact indicates that the transition at 225 K is due to transformations of the octahedral complex $Ti(O_2)F_5$. Figure 7 shows the experimental temperature dependence of the full width at half-maximum (FWHM) of the lines at 902 and 892 cm^{-1}. It is seen that, below the phase transition point T_{02}, the lines narrow fairy sharply, which demonstrates that ordering processes occur in this building block. Similar processes also take place in the group of lines at ~600 cm^{-1} corresponding to stretching vibrations of the Ti–F bonds (Fig. 4b). The conclusion that the building blocks are ordered on the phase transition at T_{02} is additionally confirmed by the existence of the "central peak" at high temperatures and its disappearance below 225 K (Fig. 4a).

To confirm our assumption that the $G_0 \longleftrightarrow G_1$ transition is associated with the ammonium-ion shifts since it is accompanied by the loss of only the triad axes, on which the ordered and disordered tetrahedral groups are arranged in the cubic lattice, we studied in detail the range of the ammonium vibrations over the temperature range 230–300 K. Figure 8 displays the temperature dependences of the frequencies of the stretching vibrations of the ammonium for the lines at 3100 and 2840 cm^{-1}. It is seen that the dependence is linear in this range. A deviation from this behavior is observed only near the transition at T_{02} = 225 K discussed above. Thus, we did not detect any anomalous behavior of the ammonium ions near the transition point T_{02} = 266 K. However, it should be noted that, at high temperatures, the lines are markedly broadened and split even in the cubic phase. Therefore, small displacements could be unnoticed against the background of the orientation disorder in these groups. In the range of the ammonium vibrations in the G_2 phase, the lines narrow and become better distinguishable; however, anomalous variations in the spectral parameters are not observed. This fact shows that the ammonium sublattice does not change substantially up to liquid-nitrogen temperature (as in the case of $(NH_4)_3TiOF_5$ [11]), in contrast to the $(NH_4)_3WO_3F_3$ compound close in structure [12, 13].

In distorted phases G_1 and G_2, the crystal studied in this work is a fairly soft ferroelectric. Deformations occurring on the first-order transition at T_{02} can influence the formed twin structure of phase G_2 on cooling and that of phase G_1 on heating. Moreover, after several repeated passages through T_{02}, the sample can become completely twin-free (Fig. 1d). We studied the influence of the mechanical state on the transition temperatures and the quality of the twinning pattern. It is established that each of the two phase transitions in both growth stress-free plates and strongly deformed plates occurs at the same temperature and has the same character. The only difference is the presence of coarser twins of the G_1 phase in the stressed plates. This is a consequence of the ferroelastic character of the PT.

4. CONCLUSIONS

Our optical studies have detected the following sequence of ferroelastic phase transitions (PTs) in the $(NH_4)_3Ti(O_2)F_5$ crystal: cubic (G_0) $\longleftrightarrow$ tetragonal (G_1) $\longleftrightarrow$ tetragonal (G_2) phase. The PT at T_{01} = 266 K exhibits the features of second-order PTs far from a critical point: $\beta = 0.50 \pm 0.01$.The loss of the triad axes is assumed to be due to the displacements of the ammonium ions arranged on them. The effects are too weak to be detected in measurements of the heat capacity [7] and in our study of the internal stretching and deformation modes of the ammonium ions. The PT at T_{02} = 225 K

observed in [7] is accompanied by an additional loss of symmetry elements, but the crystal remains tetragonal. This PT is of the first order, and the order parameter changes in a jump to a maximum value. The PT is associated with ordering inside the anion octahedral complex. The tetragonal symmetry of both the distorted phases of the crystal agrees with the structure proposed in [6, 7] for the peroxyfluoride complex $Ti(O_2)F_5$ with a dumbbell-shaped arrangement of the oxygen ions in the octahedron vertices.

ACKNOWLEDGMENTS

This work was supported by the Council on Grants from the President of the Russian Federation (project no. NSh-1011.2008.2), the Russian Foundation for Basic Research (project no. 06-02-16102), and RFBR–Eniseĭ (project no. 07-02-096800).

REFERENCES

1. W. H. Zachariasen, Acta Crystallogr. **7**, 792 (1954).
2. G. Hampson and L. Pauling, J. Am. Chem. Soc. **60**, 2702 (1938).
3. H. J. Hurst and J. C. Taylor, Acta Crystallogr., Sect. B: Struct. Crystallogr. Cryst. Chem. **26**, 417 (1970).
4. A. A. Udovenko and N. M. Laptash, Zh. Strukt. Khim. **49** (3), 498 (2008) [J. Struct. Chem. **49** (3), 482 (2008)].
5. R. Stomberg and I. B. Sveensson, Acta Chem. Scand., Ser. A **31**, 635 (1977).
6. W. Massa and G. Pausewang, Mater. Res. Bull. **13**, 361 (1970).
7. I. N. Flerov, M. V. Gorev, V. D. Fokina, M. S. Molokeev, A. D. Vasil'ev, A. F. Bovina, and N. M. Laptash, Fiz. Tverd. Tela (St. Petersburg) **48** (8), 1473 (2006) [Phys. Solid State **48** (8), 1559 (2006)].
8. K. Nakamoto, *Infrared and Raman Spectra of Inorganic and Coordination Compounds* (Wiley, New York, 1986; Mir, Moscow, 1991).
9. I. M. Iskornev, I. N. Flerov, N. F. Bezmaternykh, and K. S. Aleksandrov, Zh. Éksp. Teor. Fiz. **79** (1), 175 (1980) [Sov. Phys. JETP **52** (1), 88 (1980)].
10. V. I. Zinenko and S. V. Misyul', *Possible Phase Transitions in Crystals with the Space Group* O_h^5, Available from VINITI (November 1, 1977), No. 313-78 (1978), p. 12.
11. Yu. V. Gerasimova, A. S. Krylov, A. N. Vtyurin, N. M. Laptash, and S. V. Goryaĭnov, Fiz. Tverd. Tela (St. Petersburg) **50** (8), 1476 (2008) [Phys. Solid State **50** (8), 1534 (2008)].
12. A. N. Vtyurin, A. S. Krylov, Yu. V. Gerasimova, V. D. Fokina, N. M. Laptash, and E. I. Voĭt, Fiz. Tverd. Tela (St. Petersburg) **48** (6), 1004 (2006) [Phys. Solid State **48** (6), 1067 (2006)].
13. A. S. Krylov, Yu. V. Gerasimova, A. N. Vtyurin, V. D. Fokina, N. M. Laptash, and E. I. Voĭt, Fiz. Tverd. Tela (St. Petersburg) **48** (7), 1279 (2006) [Phys. Solid State **48** (7), 1356 (2006)].

Translated by Yu. Ryzhkov